A T-S Fuzzy Approach with Extended LMI Conditions for Inverted Pendulum on a Cart

Thi Van Anh Nguyen
School of Electrical and Electronic Engineering, Hanoi University of Science and Technology, Vietnam
anh.nguyenthivan1@hust.edu.vn (corresponding author)

Ngoc Hiep Tran
School of Electrical and Electronic Engineering, Hanoi University of Science and Technology, Vietnam
hiep.tn181466@sis.hust.edu.vn

Received: 31 October 2023 | Revised: 1 December 2023 | Accepted: 6 December 2023

 DOI: https://doi.org/10.48084/etasr.6577

ABSTRACT

The Inverted Pendulum On a Cart (IPOC) system poses a challenge in control engineering due to its inherent instability, nonlinearity, and underactuation. This addresses the fundamental issues arising from its underactuated nature and introduces an approach that combines Takagi-Sugeno (T-S) fuzzy control with an awareness of real-world constraints to create a control system ensuring both stability and practicality. By aligning theoretical insights with extended considerations, the Linear Matrix Inequality (LMI)-based control design is demonstrated in a comprehensive framework. Theorems are introduced and validated, leading to the derivation of LMI conditions. The simulation results are assessed with accompanying comments to demonstrate the effectiveness of the theorems. Through this integration of T-S fuzzy control with additional considerations, the paper aims to bridge the gap between theory and practical applications, advancing the field of control engineering.

Keywords-Takagi-Sugeno fuzzy control; inverted pendulum on a cart; linear matrix inequality; decay rate; constraint on the output

I. INTRODUCTION

The IPOC system [1-3] stands as a captivating and challenging problem within the realm of control engineering, attracting the attention of researchers and engineers. This intricate system, characterized by its inherent instability, nonlinearity, and underactuation, has long been a crucible for testing and advancing control theories. The unique appeal of the IPOC system goes beyond theoretical fascination. It extends to practical applications that touch our daily lives, from the domain of self-balancing two-wheeled vehicles [4-5] to human balance modeling [6]. This paper explores the complexity of the IPOC system, emphasizing the core challenges stemming from its underactuated nature. As an underactuated system, controlling the IPOC presents challenges. Firstly, the system has a single input, the force applied to the cart, yet it must manage two output variables: the cart position and the pendulum angle. Secondly, this system is both nonlinear and unstable, making it susceptible to collapsing even under minimal disturbances. Consequently, the implementation of control methods becomes necessary to stabilize the pendulum.

Over the years, the research community has diligently explored numerous control methods to address the challenges of this system. Control strategies like Proportional-Integral-Derivative (PID), Sliding Mode Control (SMC), Linear Quadratic Regulator (LQR), and Fuzzy Logic Control (FLC) have been examined. Authors in [7, 8] utilized LQR and a PID controller, respectively, to stabilize the inverted pendulum. In [9], the authors used the IPOC as an object to test and compare the efficiency between SMC, Integral SMC and Terminal SMC. Besides those methods, FLC [10-12], has gained attention for its ability to handle the system's nonlinearity and ensure pendulum stability. While several studies have acknowledged FLC's potential in stabilizing the pendulum in the IPOC system, many of these studies have omitted practical considerations. The real-world environment often imposes limitations, including track boundaries and stabilization time. This brings us to the core of the current research. Acknowledging the merits of FLC, the untapped potential lies in adapting this method to consider real-world conditions. This paper introduces an approach using the T-S fuzzy control [13-15] to the control design of the IPOC. The objective is to combine the strengths of T-S fuzzy control with an awareness of external constraints, such as track limits and stabilization time, in order to create a control system that not only guarantees stability, but also respects the boundaries of practical application. Authors in [16] elaborated the establishment and substantiation of stability using Lyapunov's theorem. This work is primarily concerned with achieving stability for the inverted pendulum while disregarding external factors such as track limits and stabilization time. The aim is to align theoretical insights with extended considerations. Therefore, the primary contributions of this paper include:

- Pendulum stabilization control design based on the T-S fuzzy model.
- Design of the controller with additional conditions through the LMI form.
- Result comparison and evaluation of the theorems both before and after the inclusion of additional conditions.

In this paper, the IPOC model will be introduced, stability theories both with and without the consideration of these conditions will be present, simulation results for validation and comparative analysis will be shown, and a comprehensive conclusion will be offered.

II. MODELING

The IPOC system is illustrated in the Figure 1. It includes a cart with mass denoted as m_0 and a pendulum with mass denoted as m_1. The rotation angle of the pendulum from the Y-axis is represented as φ and the connecting rod has a length denoted as l. The force that moves the cart is expressed as u, and the acceleration due to gravity is represented by g. The travel distance of the cart is denoted as x_d and the coordinates of the pendulum are denoted as $(\tilde{x}, \tilde{y})$ with $\tilde{x} = x_d + l\sin\phi$, $\tilde{y} = l\cos\phi$.

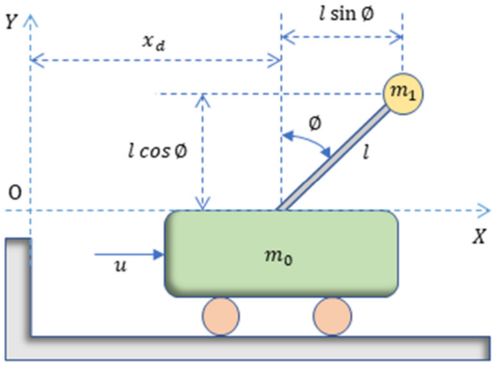

Fig. 1 Inverted pendulum on a cart.

Assuming that the mass of the connecting rod is negligible, the Lagrange equation can be obtained as:

$$\begin{aligned} L &= E_K - E_P \\ &= \frac{1}{2}(m_0 + m_1)\dot{x}_d^2 + \frac{1}{2}m_1 l^2\dot{\phi}^2 + m_1 l\dot{x}_d\dot{\phi}\cos\phi - m_1 gl\cos\phi \end{aligned} \quad (1)$$

where the system's kinetic energy and potential energy are denoted as E_K and E_P, respectively. Using the Euler-Lagrange equations:

$$\begin{aligned} &\frac{d}{dt}\left(\frac{\delta L}{\delta \dot{x}_d}\right) - \frac{\delta L}{\delta x_d} = u \\ &\frac{d}{dt}\left(\frac{\delta L}{\delta \dot{\phi}}\right) - \frac{\delta L}{\delta \phi} = 0 \end{aligned} \quad (2)$$

the dynamics equations are derived:

$$\begin{cases} (m_0 + m_1)\ddot{x}_d + m_1 l\ddot{\phi}\cos\phi - m_1 l\dot{\phi}^2\sin\phi = u \\ l\ddot{\phi} + \ddot{x}_d\cos\phi - g\sin\phi = 0 \end{cases} \quad (3)$$

After applying specific transformations, the cart position and pendulum angle dynamics are:

$$\begin{cases} \ddot{x}_d = \dfrac{-m_1 g\sin\phi\cos\phi + m_1 l\dot{\phi}^2\sin\phi + u}{m_0 + m_1\sin^2\phi} \\ \ddot{\phi} = \dfrac{(m_0 + m_1)g\sin\phi - m_1 l\dot{\phi}^2\sin\phi\cos\phi - u\cos\phi}{l(m_0 + m_1\sin^2\phi)} \end{cases} \quad (4)$$

III. CONTROL DESIGN

A. *The Takagi-Sugeno Fuzzy Model*

The T-S fuzzy model depicts a nonlinear system through its division into subsystems. Each subsystem is described using a local linear input-output relation through an IF-THEN rule. The overall system is derived by synthesizing the linear system models as follows:

$$\begin{cases} \dot{x}(t) = \sum_{i=1}^{r} n_i(s(t))(A_i x(t) + B_i u(t)) \\ y(t) = \sum_{i=1}^{r} n_i(s(t))C_i x(t) \end{cases} \quad i = 1,2,\ldots,r \quad (5)$$

where the system's state vector is denoted as $x(t)$, the input vector is represented as $u(t)$, the output vector is described by $y(t)$, A_i, B_i, C_i are subsystem matrices, r is the number of rules, and $n_i(s(t))$ represents the membership functions, which, with their convex sum property, are defined as:

$$\begin{aligned} &n_i(s(t)) = \frac{w_i(s(t))}{\sum_{i=1}^{r} w_i(s(t))} \\ &\begin{cases} \sum_{i=1}^{r} w_i(s(t)) > 0 \\ w_i(s(t)) \geq 0 \end{cases} \quad i = 1,2,\ldots,r \end{aligned} \quad (6)$$

where $s = \begin{bmatrix} s_1 & s_2 & \ldots & s_p \end{bmatrix}$ is a premise variables vector, p is the number of premise variables such that $r = 2^p$, and $w_i(s(t))$ are calculated by:

$$w_{i0} = \frac{s_{i\max} - s_i}{s_{i\max} - s_{i\min}}, \quad w_{i1} = 1 - w_{i0}, \quad i = 1,2,\ldots,p \quad (7)$$

Applying to the IPOC system, the premise variables are defined as:

$$\begin{aligned} &s_1 = \frac{1}{m_0 + m_1\sin^2\phi}, \quad s_2 = \cos\phi \\ &s_3 = \frac{\sin\phi}{\phi}, \quad s_4 = \dot{\phi}\sin\phi \end{aligned} \quad (8)$$

The system's state equation takes the following form:

$$\dot{x} = Ax + Bu \tag{9}$$

where:

$$x = \begin{bmatrix} x_d & \dot{x}_d & \phi & \dot{\phi} \end{bmatrix}$$

$$A = \begin{bmatrix} 0 & 1 & 0 & 0 \\ 0 & 0 & -m_1 g s_1 s_2 s_3 & m_1 l s_1 s_3 s_4 \\ 0 & 0 & 0 & 1 \\ 0 & 0 & \dfrac{(m_0+m_1) g s_1 s_2}{l} & -m_1 s_1 s_2 s_3 s_4 \end{bmatrix}$$

$$B = \begin{bmatrix} 0 \\ s_1 \\ 0 \\ \dfrac{-s_1 s_2}{l} \end{bmatrix}$$

B. LMI-based Control Design

Upon constructing the T-S fuzzy model, the Parallel Distributed Compensation (PDC) [17] is structured to calculate the control signal $u(t)$. Each subsystem has a control rule corresponding to its T-S model. The fuzzy controller is designed using the identical fuzzy set as the premise part of the fuzzy model. With K_i being the feedback gain of the i^{th} subsystem, the overall PDC can be obtained as:

$$u(t) = -\sum_{i=1}^{r} n_i(s(t)) K_i x(t) \cdot \tag{10}$$

The PDC is derived through theorems in the form of linear matrix inequality. Some abbreviations used in the LMI context are: I is the identity matrix, $Q > 0$, $\alpha > 0$, $\lambda > 0$, $Z = Q^{-1}$, $G_i = K_i Z$. To design a controller with the aim of stabilizing the system, the following theorems should be held:

1) Theorem 1 [16]: Stability Conditions

The fuzzy system (5) achieves globally asymptotically stability when there is a common positive definite matrix Z such that:

$$\begin{cases} -ZA_i^{\mathrm{T}} - A_i Z + G_i^{\mathrm{T}} B_i^{\mathrm{T}} + B_i G_i > 0 \\ -ZA_i^{\mathrm{T}} - A_i Z - ZA_j^{\mathrm{T}} - A_j Z \\ +G_j^{\mathrm{T}} B_i^{\mathrm{T}} + B_i G_j + G_i^{\mathrm{T}} B_j^{\mathrm{T}} + B_j G_i \geq 0 \end{cases} \tag{11}$$

Proof:

A Lyapunov function $V(x(t)) = x^{\mathrm{T}}(t) Q x(t)$ is chosen. For the system (5) to achieve global asymptotic stability, the following condition must be satisfied:

$$\dot{V}(x(t)) < 0$$

$$\Leftrightarrow \dot{x}^{\mathrm{T}}(t) Q x(t) + x^{\mathrm{T}}(t) Q \dot{x}(t) < 0$$

$$\Leftrightarrow (A_i - B_i K_j)^{\mathrm{T}} Q + Q(A_i - B_i K_j) < 0$$

$$\Leftrightarrow \begin{cases} -(A_i - B_i K_i)^{\mathrm{T}} Q - Q(A_i - B_i K_i) > 0 \\ -\dfrac{(A_i - B_i K_j)^{\mathrm{T}} + (A_j - B_j K_i)^{\mathrm{T}}}{2} Q - \\ Q \dfrac{(A_i - B_i K_j) + (A_j - B_j K_i)}{2} \geq 0 \end{cases} \tag{12}$$

Multiplying on both sides of (12) with Z results in:

$$\Leftrightarrow \begin{cases} -ZA_i^{\mathrm{T}} - A_i Z + G_i^{\mathrm{T}} B_i^{\mathrm{T}} + B_i G_i > 0 \\ -ZA_i^{\mathrm{T}} - A_i Z - ZA_j^{\mathrm{T}} - A_j Z \\ +G_j^{\mathrm{T}} B_i^{\mathrm{T}} + B_i G_j + G_i^{\mathrm{T}} B_j^{\mathrm{T}} + B_j G_i \geq 0 \end{cases}$$

This concludes the proof.

2) Theorem 2: Stability Conditions, Decay Rate, and Constraint on the Output

Regarding the IPOC system, stabilizing the inverted pendulum in an upright position is insufficient. Practical considerations, like constraining the cart position or stabilization time of the pendulum, come into play. Therefore, theorem 2 will be introduced to account for these additional conditions.

- Stability conditions:

$$\begin{cases} -ZA_i^{\mathrm{T}} - A_i Z + G_i^{\mathrm{T}} B_i^{\mathrm{T}} + B_i G_i > 0 \\ -ZA_i^{\mathrm{T}} - A_i Z - ZA_j^{\mathrm{T}} - A_j Z \\ +G_j^{\mathrm{T}} B_i^{\mathrm{T}} + B_i G_j + G_i^{\mathrm{T}} B_j^{\mathrm{T}} + B_j G_i \geq 0 \end{cases} \tag{13}$$

- Decay rate: The response's speed is related to decay rate. Maximize α subject to:

$$\begin{cases} -ZA_i^{\mathrm{T}} - A_i Z + G_i^{\mathrm{T}} B_i^{\mathrm{T}} + B_i G_i - 2\alpha Z > 0 \\ -ZA_i^{\mathrm{T}} - A_i Z - ZA_j^{\mathrm{T}} - A_j Z \\ +G_j^{\mathrm{T}} B_i^{\mathrm{T}} + B_i G_j + G_i^{\mathrm{T}} B_j^{\mathrm{T}} + B_j G_i - 4\alpha Z \geq 0 \end{cases} \tag{14}$$

Proof:

We chose a Lyapunov function as $V(x(t)) = x^{\mathrm{T}}(t) Q x(t)$.

From the condition that $\dot{V}(x(t)) \leq -2\alpha V(x(t))$, this is equivalent to:

$$\dot{x}^{\mathrm{T}}(t)(A_i - B_i K_j)^{\mathrm{T}} Q x(t) + x^{\mathrm{T}}(t) Q (A_i - B_i K_j) x(t)$$

$$+2\alpha x^{\mathrm{T}}(t) Q x(t) \leq 0$$

$$\Leftrightarrow (A_i - B_i K_j)^{\mathrm{T}} Q + Q(A_i - B_i K_j) + 2\alpha Q \leq 0$$

Following stability conditions in theorem 1, it is inferred:

$$\Leftrightarrow \begin{cases} -A_i^{\mathrm{T}} Q - QA_i + K_i^{\mathrm{T}} B_i^{\mathrm{T}} Q + QB_i K_i - 2\alpha Q > 0 \\ -A_i^{\mathrm{T}} Q - QA_i - A_j^{\mathrm{T}} Q - QA_j + K_j^{\mathrm{T}} B_i^{\mathrm{T}} Q + QB_i K_j \\ +K_i^{\mathrm{T}} B_j^{\mathrm{T}} Q + QB_j K_i - 4\alpha Q \geq 0 \end{cases} \tag{15}$$

Multiplying Z on both sides of (15), then (14) is obtained:

$$\begin{cases} -ZA_i^{\mathrm{T}} - A_i Z + G_i^{\mathrm{T}} B_i^{\mathrm{T}} + B_i G_i - 2\alpha Z > 0 \\ -ZA_i^{\mathrm{T}} - A_i Z - ZA_j^{\mathrm{T}} - A_j Z \\ +G_j^{\mathrm{T}} B_i^{\mathrm{T}} + B_i G_j + G_i^{\mathrm{T}} B_j^{\mathrm{T}} + B_j G_i - 4\alpha Z \geq 0 \end{cases}$$

- Constraint on the output: With the assumption of knowing the initial condition $x(0)$, the constraint $\|y(t)\|_2 \leq \lambda$ is held if these LMIs are satisfied:

$$\begin{bmatrix} 1 & x(0)^{\mathrm{T}} \\ x(0) & Z \end{bmatrix} \geq 0 \tag{16}$$

$$\begin{bmatrix} Z & ZC_i^{\mathrm{T}} \\ C_i Z & \lambda^2 I \end{bmatrix} \geq 0 \tag{17}$$

Proof: Following [17]. A Lyapunov function is chosen as $V(x(t)) = x^{\mathrm{T}}(t)Qx(t)$ and assuming that:

$$x^{\mathrm{T}}(0)Qx(0) \leq 1. \tag{18}$$

From $\|y(t)\|_2 \leq \lambda$, it can be inferred that:

$$y^{\mathrm{T}}(t)y(t) = \sum_{i=1}^{r}\sum_{j=1}^{r} n_i(s(t))n_j(s(t))x^{\mathrm{T}}(t)C_i^{\mathrm{T}}C_j x(t) \leq \lambda^2$$

$$\Leftrightarrow \frac{1}{\lambda^2}\sum_{i=1}^{r}\sum_{j=1}^{r} n_i(s(t))n_j(s(t))x^{\mathrm{T}}(t)C_i^{\mathrm{T}}C_j x(t) \leq 1$$

Since $x^{\mathrm{T}}(t)Z^{-1}x(t) < x^{\mathrm{T}}(0)Z^{-1}x(0) \leq 1 \; \forall t > 0$, the above equation holds if:

$$\frac{1}{\lambda^2}\sum_{i=1}^{r}\sum_{j=1}^{r} n_i(s(t))n_j(s(t))x^{\mathrm{T}}(t)C_i^{\mathrm{T}}C_j x(t) \leq x^{\mathrm{T}}(t)Z^{-1}x(t)$$

$$\Leftrightarrow \sum_{i=1}^{r}\sum_{j=1}^{r} n_i(s(t))n_j(s(t))x^{\mathrm{T}}(t)\left(\frac{1}{\lambda^2}C_i^{\mathrm{T}}C_j - Z^{-1}\right)x(t) \leq 0$$

From the left side of the above equation:

$$\frac{1}{2}\sum_{i=1}^{r}\sum_{j=1}^{r} n_i(s(t))n_j(s(t))x^{\mathrm{T}}(t)\left(\frac{1}{\lambda^2}C_i^{\mathrm{T}}C_j + \frac{1}{\lambda^2}C_j^{\mathrm{T}}C_i - 2Z^{-1}\right)x(t)$$

$$= \frac{1}{2}\sum_{i=1}^{r}\sum_{j=1}^{r} n_i(s(t))n_j(s(t))x^{\mathrm{T}}(t)\times$$

$$\left[\frac{1}{\lambda^2}\left(C_i^{\mathrm{T}}C_i + C_j^{\mathrm{T}}C_j\right) - \frac{1}{\lambda^2}\left(C_i^{\mathrm{T}} - C_j^{\mathrm{T}}\right)\left(C_i - C_j\right) - 2Z^{-1}\right]x(t)$$

$$\leq \frac{1}{2}\sum_{i=1}^{r}\sum_{j=1}^{r} n_i(s(t))n_j(s(t))x^{\mathrm{T}}(t)\times\left[\frac{1}{\lambda^2}\left(C_i^{\mathrm{T}}C_i + C_j^{\mathrm{T}}C_j\right) - 2Z^{-1}\right]x(t)$$

$$= \sum_{i=1}^{r} n_i(s(t))x^{\mathrm{T}}(t)\left(\frac{1}{\lambda^2}C_i^{\mathrm{T}}C_i - Z^{-1}\right)x(t)$$

So, $\|y(t)\|_2 \leq \lambda$ holds if:

$$\frac{1}{\lambda^2}C_i^{\mathrm{T}}C_i - Z^{-1} \leq 0 \tag{19}$$

Multiplying Z on both sides of (19):

$$\frac{1}{\lambda^2}ZC_i^{\mathrm{T}}C_i Z - Z \leq 0 \tag{20}$$

Using the Schur complement procedure for (18) and (20), LMI conditions (16) and (17) are derived.

By employing theorem 1 to the IPOC system, stability is achieved. Even though the inverted pendulum is maintained in a vertical position, the dynamics of the system requires additional conditions due to practical limitations. The length of the cart track is being limited and the stability duration should be kept relatively short. Consequently, theorem 2 is more applicable into this system. To validate the effectiveness of both theorems as well as demonstrate the superior performance of theorem 2 compared to theorem 1, the simulation results will be presented in the following section.

IV. SIMULATION

The parameters for simulation are chosen as: m_0 =1.5 kg, m_1 =0.3 kg, l = 0.3 m, g =0.3 m/s^2. The system's initial conditions are: $x(0) = [x_{d0} \quad \dot{x}_{d0} \quad \phi_0 \quad \dot{\phi}_0]$, $x_{d0} = 0$, $\dot{x}_{d0} = 0$, $\phi_0 = \frac{\pi}{6}$ (rad), $\dot{\phi} = 0$. The boundaries are $\frac{-\pi}{3} \leq \phi \leq \frac{\pi}{3}$ (rad), $-6 \leq \dot{\phi} \leq 6$ (rad/s). Additionally, the parameters in theorem 2 are given as a = *0.9*, λ = 7. The calculated values of $s_{i\ \max}$ and $s_{i\ \min}$ are shown in Table I.

TABLE I. PREMISE VARIABLES VALUES

i	$s_{i\ \max}$	$s_{i\ \min}$
1	0.6667	0.5797
2	1	0.5
3	1	0.827
4	5.1962	-5.1962

The simulation results when employing both theorems are shown in Figures 2-6. The blue line depicts the system's states and control signal for theorem 1, whereas the red line represents those for theorem 2. Figures 2 and 3 illustrate cart position and cart velocity, respectively. The pendulum angle is described in Figure 4 and the pendulum angle velocity is shown in Figure 5. Figure 6 presents the control signal.

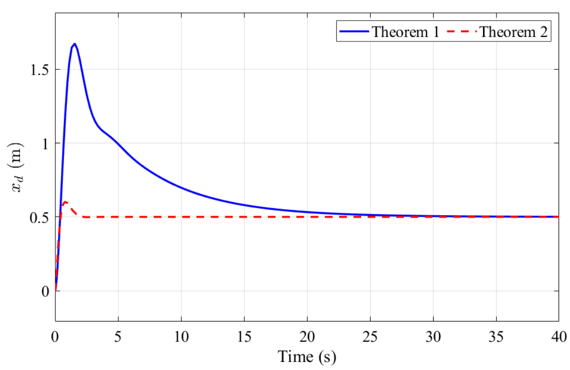

Fig. 2 Cart position.

In Figure 2, the position of the cart under theorem 1 and theorem 2 are compared and the difference is evident. The results show that theorem 2 achieves a significantly faster cart position stabilization time (approximately 2 s) compared to theorem 1 (about 30 s). It's worth noting that the cart position response curve for theorem 2 reaches a maximum value of approximately 0.6 m, whereas under theorem 1, this maximum value is as high as 1.7 m. This confirms the earlier assertion that theorem 2 provides results that align more closely with real mechanical constraints.

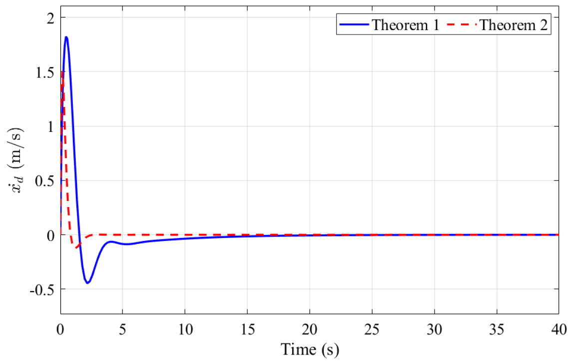

Fig. 3 Cart velocity.

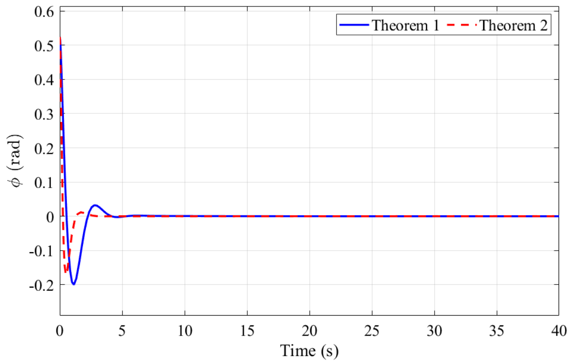

Fig. 4 Pendulum angle.

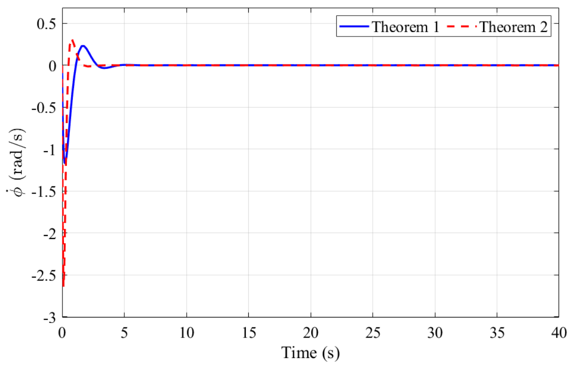

Fig. 5 Pendulum angle velocity.

Similar to the cart position results, the pendulum angle also exhibits faster stabilization when applying theorem 2 compared to theorem 1 (2.5 s compared to 5 s), as shown in Figure 4. Once again, these results further bolster the points mentioned earlier. In Figures 3 and 5, respectively, the speed of the cart and the angular speed of the inverted pendulum are shown for both theorems. Although there are differences between the results, these state variables remain within the prescribed limits. Figure 6 illustrates the force acting on the cart, reflecting a subjective judgment aimed at finely regulating the system's dynamics. This translates to a higher energy exchange. Consequently, the force applied to the cart in theorem 2 is greater than that in theorem 1.

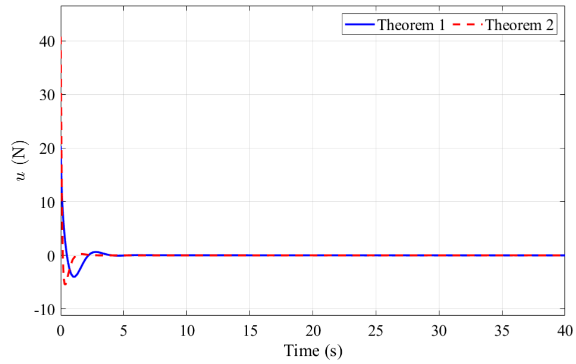

Fig. 6 Control signal.

V. CONCLUSION

This paper presents the control design through two theorems and their application to the inverted pendulum on a cart system. Simulation results have been presented after introducing the theorems and proving their effectiveness, highlighting the superiority of theorem 2 over theorem 1. This research represents a significant step towards applying these theorems to control design for experimental systems, potentially contributing to advancements in control engineering.

ACKNOWLEDGMENT

This research is funded by Hanoi University of Science and Technology (HUST) under project number T2023-PC-036.

REFERENCES

[1] S. Hadipour Lakmesari, M. J. Mahmoodabadi, and M. Yousef Ibrahim, "Fuzzy logic and gradient descent-based optimal adaptive robust controller with inverted pendulum verification," *Chaos, Solitons & Fractals*, vol. 151, Oct. 2021, Art. no. 111257, https://doi.org/10.1016/j.chaos.2021.111257.

[2] E. Susanto, A. Surya Wibowo, and E. Ghiffary Rachman, "Fuzzy Swing Up Control and Optimal State Feedback Stabilization for Self-Erecting Inverted Pendulum," *IEEE Access*, vol. 8, pp. 6496–6504, 2020, https://doi.org/10.1109/ACCESS.2019.2963399.

[3] T. Johnson, S. Zhou, W. Cheah, W. Mansell, R. Young, and S. Watson, "Implementation of a Perceptual Controller for an Inverted Pendulum Robot," *Journal of Intelligent & Robotic Systems*, vol. 99, no. 3, pp. 683–692, Sep. 2020, https://doi.org/10.1007/s10846-020-01158-4.

[4] S.-J. Huang, S.-S. Chen, and S.-C. Lin, "Design and Motion Control of a Two-Wheel Inverted Pendulum Robot," *International Journal of Mechanical and Mechatronics Engineering*, vol. 13, no. 3, pp. 194–201, Feb. 2019, https://doi.org/10.5281/zenodo.2643591.

[5] G. Curiel-Olivares, J. Linares-Flores, J. F. Guerrero-Castellanos, and A. Hernández-Méndez, "Self-balancing based on Active Disturbance

Rejection Controller for the Two-In-Wheeled Electric Vehicle, Experimental results," *Mechatronics*, vol. 76, Jun. 2021, Art. no. 102552, https://doi.org/10.1016/j.mechatronics.2021.102552.

[6] T. Zielinska, G. R. R. Coba, and W. Ge, "Variable Inverted Pendulum Applied to Humanoid Motion Design," *Robotica*, vol. 39, no. 8, pp. 1368–1389, Aug. 2021, https://doi.org/10.1017/S0263574720001228.

[7] M. A. Sen and M. Kalyoncu, "Optimal Tuning of a LQR Controller for an Inverted Pendulum Using the Bees Algorithm," *Journal of Automation and Control Engineering*, pp. 384–387, 2016, https://doi.org/10.18178/joace.4.5.384-387.

[8] B. Abeysekera and W. K. Wanniarachchi, "Modelling and Implementation of PID Control for Balancing of an Inverted Pendulum," *International Journal of Automation, Control and Intelligent Systems*, vol. 4, no. 4, pp. 43–53, Dec. 2018.

[9] S. Irfan, A. Mehmood, M. T. Razzaq, and J. Iqbal, "Advanced sliding mode control techniques for Inverted Pendulum: Modelling and simulation," *Engineering Science and Technology, an International Journal*, vol. 21, no. 4, pp. 753–759, Aug. 2018, https://doi.org/10.1016/j.jestch.2018.06.010.

[10] G. S. Maraslidis, T. L. Kottas, M. G. Tsipouras, and G. F. Fragulis, "Design of a Fuzzy Logic Controller for the Double Pendulum Inverted on a Cart," *Information*, vol. 13, no. 8, Aug. 2022, Art. no. 379, https://doi.org/10.3390/info13080379.

[11] B. Kasmi and A. Hassam, "Comparative Study between Fuzzy Logic and Interval Type-2 Fuzzy Logic Controllers for the Trajectory Planning of a Mobile Robot," *Engineering, Technology & Applied Science Research*, vol. 11, no. 2, pp. 7011–7017, Apr. 2021, https://doi.org/10.48084/etasr.4031.

[12] S. Hadipour Lakmesari, M. J. Mahmoodabadi, and M. Yousef Ibrahim, "Fuzzy logic and gradient descent-based optimal adaptive robust controller with inverted pendulum verification," *Chaos, Solitons & Fractals*, vol. 151, Oct. 2021, Art. no. 111257, https://doi.org/10.1016/j.chaos.2021.111257.

[13] I. H. Hamad, A. Chouchaine, and H. Bouzaouache, "A Takagi-Sugeno Fuzzy Model for Greenhouse Climate," *Engineering, Technology & Applied Science Research*, vol. 11, no. 4, pp. 7424–7429, Aug. 2021, https://doi.org/10.48084/etasr.4291.

[14] N. V. Hai, N. V. Tiem, L. H. Lan, and T. H. Vo, "Pantograph Catenary Contact Force Regulation Based on Modified Takagi-Sugeno Fuzzy Models," *Engineering, Technology & Applied Science Research*, vol. 13, no. 1, pp. 9879–9887, Feb. 2023, https://doi.org/10.48084/etasr.5443.

[15] R. V. Gandhi and D. M. Adhyaru, "Takagi-Sugeno fuzzy regulator design for nonlinear and unstable systems using negative absolute eigenvalue approach," *IEEE/CAA Journal of Automatica Sinica*, vol. 7, no. 2, pp. 482–493, Mar. 2020, https://doi.org/10.1109/JAS.2019.1911444.

[16] A. I. Roose, S. Yahya, and H. Al-Rizzo, "Fuzzy-logic control of an inverted pendulum on a cart," *Computers & Electrical Engineering*, vol. 61, pp. 31–47, Jul. 2017, https://doi.org/10.1016/j.compeleceng.2017.05.016.

[17] K. Tanaka and H. O. Wang, *Fuzzy Control Systems Design and Analysis: A Linear Matrix Inequality Approach*. John Wiley & Sons, Ltd, 2001.